



# Molecular mechanism underlying anti-inflammatory activities of liriioresinol B dimethyl ether through suppression of NF- $\kappa$ B and MAPK signaling in *in vitro* and *in vivo* models

Yunshu Su<sup>\*\*</sup>, Sizheng Xiong, Hongwen Lan, Lijun Xu<sup>\*</sup>, Xiang Wei<sup>\*</sup>

Department of Cardiothoracic and Vascular Surgery, Tongji Hospital, Tongji Medical College, Huazhong University of Science and Technology, Wuhan 430030, PR China

## ARTICLE INFO

### Keywords:

Liriioresinol B dimethyl ether  
Anti-inflammatory  
MAPKs/AP-1  
NF- $\kappa$ B  
Carrageenan

## ABSTRACT

The aim of the present study is to explore the anti-inflammatory mechanism of liriioresinol B dimethyl ether *in vitro* and *in vivo* pharmacological models. To determine the anti-inflammatory activity of the liriioresinol B dimethyl ether, RAW 264.7 macrophages challenged with lipopolysaccharide (LPS) were treated with various concentrations of liriioresinol B dimethyl ether (5, 15, 25, and 50  $\mu$ M). The results indicated that pretreatment with liriioresinol B dimethyl ether significantly suppressed nuclear factor kappa B (NF- $\kappa$ B) activation, nitric oxide (NO) production, the protein expressions of inducible nitric oxide synthase (iNOS) and cyclooxygenase-2 (COX-2). Liriioresinol B dimethyl ether inhibited LPS-induced activation of production of pro-inflammatory cytokines as well as prostaglandin E<sub>2</sub> (PGE<sub>2</sub>) release. The results obtained by electrophoretic mobility shift assay (EMSA) demonstrated a concentration dependent reduction of the LPS-stimulated activation of NF- $\kappa$ B and activator protein-1 (AP-1) by liriioresinol B dimethyl ether in *in vitro* and *in vivo* models. Moreover, liriioresinol B dimethyl ether also reduced the expression of toll-like receptor (TLR)-4 protein and myeloid differentiation primary response gene 88 (MyD88) as well as promoted the degradation of  $\kappa$ B $\alpha$ . Liriioresinol B dimethyl ether also significantly down-regulated the phosphorylation of Jun N-terminal kinase (JNK), p-38 and extracellular signal-regulated kinase (ERK). Furthermore, the results of acute and chronic inflammation demonstrated that liriioresinol B dimethyl ether (10 and 50 mg per kg) reduced paw edema and mechanical hyperalgesia in carrageenan- and Complete Freund's Adjuvant (CFA)-induced *in vivo* mouse models, respectively. Hence, the current results indicate that liriioresinol B dimethyl ether either act by inhibiting pro-inflammatory mediators through down-regulation of mitogen activated protein kinases (MAPKs) signaling pathways and reduction of NF- $\kappa$ B activation.

## 1. Introduction

Inflammation is the first line of defense against pathogen invasion, characterized by redness, heat, swelling, pain and loss of various functions [1]. Acute or chronic inflammation leads to inflammatory diseases, such as sepsis, atherosclerosis, rheumatoid arthritis, cancer, and diabetes [2]. Inflammatory responses defend the body against various physical or chemical traumas, triggering immunobiological events that result in the production of chemokines, cytokines, and pro-inflammatory mediators, such as prostaglandin E<sub>2</sub> (PGE<sub>2</sub>) and nitric oxide (NO) [3,4]. Numerous studies have elucidated the underlying molecular mechanism associated with the pathological process of

inflammation induced by various stimuli [5]. Specific intracellular signaling molecules present a possible target for the prevention and cure of inflammatory diseases. Various natural compounds have successfully exerted anti-inflammatory effects by targeting intracellular molecules involved in inflammatory cascades.

Inflammatory responses are governed by innate immune cells, such as macrophages, dendritic cells, or neutrophils involved in the recognition of pathogen-associated molecular patterns (PAMPs) through a panel of conserved pattern-recognition receptors (PRRs) and toll-like receptors (TLRs) [6,7]. Toll-like receptor 4 (TLR4), a member of the TLR family, is recognized and activated by a major component of Gram-negative bacteria, *i.e.*, lipopolysaccharide (LPS) [8]. Myeloid

<sup>\*</sup> Corresponding authors at: Department of Cardiothoracic and Vascular Surgery, Tongji Hospital, Tongji Medical College, Huazhong University of Science and Technology, No.1095 Jiefang Avenue, Wuhan 430030, PR China.

<sup>\*\*</sup> Correspondence to: Y. Su, Department of Cardiothoracic and Vascular Surgery, Tongji Hospital, Tongji Medical College, Huazhong University of Science and Technology, No.1095 Jiefang Avenue, Wuhan 430030, PR China.

E-mail addresses: [micxu@163.com](mailto:micxu@163.com) (Y. Su), [n803ve@163.com](mailto:n803ve@163.com) (L. Xu), [xiangwei201808@163.com](mailto:xiangwei201808@163.com) (X. Wei).

<https://doi.org/10.1016/j.intimp.2019.05.020>

Received 26 March 2019; Received in revised form 15 April 2019; Accepted 10 May 2019

Available online 23 May 2019

1567-5769/© 2019 Elsevier B.V. All rights reserved.

differentiation primary response gene (88) (MyD88) is involved in independent and dependent pathways stimulated by the signaling cascades activated by LPS featuring nuclear factor-kappa B (NF- $\kappa$ B) and mitogen-activated protein kinase (MAPKs) pathway activation [9]. Activated macrophages produce pro-inflammatory mediators, such as NO produced by inducible nitric oxide synthase (iNOS) and PGE<sub>2</sub> produced by cyclooxygenase-2 (COX-2) proteins and cytokines, like TNF- $\alpha$ , interleukin (IL)-6, and IL-1 $\beta$  [10,11]. Various stimuli act *via* distinct signaling pathways for the activation of I $\kappa$ B kinase (IKK), initiating I $\kappa$ B phosphorylation resulting in ubiquitination, thus releasing NF- $\kappa$ B dimers from the complex of NF- $\kappa$ B-I $\kappa$ B and allowing free translocation of NF- $\kappa$ B into the nucleus [12]. Physical and chemical stress activates the MAPK family, *i.e.*, p38 MAPK, c-Jun NH2-terminal kinase (JNK), and extracellular signal regulated kinase (ERK). These regulate immune responses and express inflammatory cytokines [13,14].

Lirioresinol B dimethyl ether is a tetrahydrofuranoid lignin derived from the flower buds of *Magnoliae Flos*. It belongs to the family, Magnoliaceae, traditionally known to treat allergic rhinitis and sinusitis. *Magnoliae* spp. are listed in the Chinese, Korean, and Japanese Pharmacopoeias. [15]. The tetrahydrofuranoid lignans have been reported as primary active compounds of *Magnoliae Flos* [16,17]. Lirioresinol B dimethyl ether has been reported to have anti-microbial and anti-cancer activities [18,19]. In the present study, we aimed to evaluate the preventive and therapeutic potential of lirioresinol B dimethyl ether against many inflammatory diseases through utilizing *in vitro* and *in vivo* inflammatory conditions and models.

## 2. Materials and methods

### 2.1. Chemicals and reagents

LPS, dexamethasone, parthenolide, phosphate-buffered saline (PBS), carrageenan, Tween 20, benzamethonium chloride, EDTA, and phenylmethylsulfonyl fluoride (PMSF) were purchased from Sigma-Aldrich (Steinheim, Germany). Lirioresinol B dimethyl ether was purchased from Rochem Pharma. Co., Ltd. (China). All of the antibodies were obtained from Santa Cruz Biotechnology (Santa Cruz, CA).

### 2.2. Animals

In the present study, male Swiss albino mice (Wuhan, China) 3–4 weeks of age were obtained. They were acclimated for 1–2 weeks and then utilized for experiment at the age of 4–6 weeks, weighing 25–30 g. All animal studies were performed in a pathogen-free animal laboratory according to Huazhong University of Science and Technology Guide for the Care and Use of Laboratory Animals. The animals were kept at 23  $\pm$  0.5 °C in a 12-h light/dark cycle with 50  $\pm$  10% relative humidity. The animals were randomly divided into separate groups containing seven mice each.

### 2.3. Cells and culture medium

Murine macrophages RAW 264.7 were purchased from the American Type Culture Collection (Manassas, VA) and maintained within an appropriate atmosphere. Sub-culturing and culturing was performed [20] and a 100 mM stock concentration for all the samples was prepared in dimethyl sulfoxide (DMSO) and further dilution was carried out for working concentrations. To avoid interference with the assay, the final DMSO concentration was < 0.2%.

### 2.4. The MTT assay for determination of cell viability

An MTT (4, 5-dimethylthiazol-2-yl)-2,5-diphenyl tetrazolium bromide) assay was performed for the determination of cell viability of lirioresinol B dimethyl ether, carried according to Khan et al. [21]. Briefly, RAW 264.7 cells were plated at a density of 1  $\times$  10<sup>5</sup> per well in

a 24-well plate and incubated at 37 °C for 24 h. The cells were treated with various concentrations (5, 15, 25, and 50  $\mu$ M) of lirioresinol B dimethyl ether or vehicle alone or positive control *N*-p-tosyl-L-phenylalanyl chloromethyl ketone (TPCK, 30  $\mu$ M) for 2 h before LPS (1  $\mu$ g/ml) stimulation and then incubated at 37 °C for an additional 20 h. The NO assay was performed according to Griess reagent methods [21].

### 2.5. Western immunoblot analysis

Western blot analysis was performed according to the manufacturer's instructions for the determination of total protein by pre-treating RAW 264.7 macrophages with indicated concentrations of lirioresinol B dimethyl ether or vehicle 2 h prior to stimulation with 1  $\mu$ g per ml LPS for 30 min. A total of 10  $\mu$ g of protein for iNOS, p-p38, p38, I $\kappa$ B $\alpha$ , phosphor-I $\kappa$ B $\alpha$ , p-ERK, ERK, p-JNK, JNK, p65, p50, and 5  $\mu$ g of COX-2 were separated by SDS-PAGE, 8% (iNOS, and COX-2) and 10% (I $\kappa$ B $\alpha$ , and phosphor-I $\kappa$ B $\alpha$ , p-ERK, MyD88, p-p38, p-JNK, TIRAP, COX-2, and iNOS). Based on the manufacturer's protocol, the proteins were electro-transferred after electrophoresis to a nitrocellulose membrane (Whatman GmbH, Dassel, Germany), blocked with 5% non-fat milk in TBS-T buffer, and blotted with primary antibody and its corresponding secondary antibody. The WEST-SAVE Up™ luminol-based ECL reagent (LabFrontier, Seoul, Korea) was employed for the detection of antibodies and the target bands were quantified *via* UN-SCAN-IT™ software, version 6.1 (Silk Scientific Co., Orem, UT). Similarly, Western blotting was performed in CFA-induced paw tissue as described elsewhere [21,22].

### 2.6. NF- $\kappa$ B secretory alkaline phosphatase (SEAP) reporter gene assay in transfected-RAW 264.7 cells

The NF- $\kappa$ B SEAP inhibitory activity of lirioresinol B dimethyl ether was analyzed in RAW 264.7 macrophages stimulated with LPS by the SEAP assay, as described previously [21–23]. In brief, 1  $\times$  10<sup>5</sup> RAW 264.7 macrophages were transfected with pNF- $\kappa$ B-SEAP-NPT, the encoding - $\kappa$ B sequence (four copies), and the SEAP gene as a reporter, and these were all pre-incubated with lirioresinol B dimethyl ether at different concentrations for 2 h and then challenged with LPS (1 mg/ml) for an additional 20 h. The positive control used in this experiment was *N*-p-tosyl-L-phenylalanyl chloromethyl ketone (TPCK, 30  $\mu$ M).

### 2.7. Electrophoretic mobility shift assay (EMSA) in LPS-induced RAW macrophages

EMSA was performed in order to explore the inhibitory effect of lirioresinol B dimethyl ether on DNA binding of AP-1 and NF- $\kappa$ B as described previously [21–23]. The quantification of signals obtained from the dried gel was carried out with an FLA-3000 apparatus (Fuji) utilizing the BAS reader, version 3.14, and Aida, version 3.22, software (Amersham Biosciences, Piscataway, USA). The binding conditions were optimized as reported earlier. The NF- $\kappa$ B DNA-binding affinity was determined in CFA-induced paw tissue as described elsewhere [21,22].

### 2.8. Determination of PGE<sub>2</sub> levels in RAW 264.7 cells

The PGE<sub>2</sub> levels were measured with a standard enzyme immunoassay (EIA) kit for PGE<sub>2</sub> from activated macrophages according to the manufacturer's recommendations (Cayman Chemical, Ann Arbor, USA). Briefly, 1  $\times$  10<sup>5</sup> cells were seeded in 24-well plates for 24 h. Cells were pre-treated with several concentrations of lirioresinol B dimethyl ether or a vehicle for 2 h and then the macrophages were stimulated by LPS (1  $\mu$ g/ml) for an additional 18 h. 100  $\mu$ l of the supernatant was transferred to 96-well culture plate and PGE<sub>2</sub> was determined according to the manufacturer's instructions (Cayman Chemical, Ann Arbor, USA). Absorbance at 405 nm was recorded with a microplate reader

(Molecular Devices, Emax, Sunnyvale, USA). For comparison, 50  $\mu\text{M}$  of celecoxib (Celebrex®, Pfizer, New York, USA) was used as a positive control [24].

### 2.9. Determination of nitric oxide levels in RAW 264.7 cells

Nitrite concentration in the medium was measured as an indicator of nitric oxide production according to the Griess method. In a 24-well plate,  $1 \times 10^5$  RAW264.7 cells were plated, incubated for 24 h, and pre-treated with liriorelinol B dimethyl ether (5, 15, 25, 50  $\mu\text{M}$ ) or a vehicle for another 2 h, then challenged with LPS (1  $\mu\text{g}/\text{ml}$ ) for an additional 18 h. Equal volumes of Griess reagent and culture medium were mixed, and the absorbance was determined at 540 nm with a microplate reader (Molecular Devices, Emax, Sunnyvale, USA). The absorption coefficient was calibrated with a sodium nitrite solution standard. For this experiment, *N*-p-tosyl-L-phenylalanyl chloromethyl ketone (TPCK, 30  $\mu\text{M}$ ) was used as a positive control.

### 2.10. Measurement of pro-inflammatory cytokine production

To determine the inhibitory effect of liriorelinol B dimethyl ether on the production of pro-inflammatory cytokines (TNF- $\alpha$ , IL-1 $\beta$  and IL-6) in the culture medium, cells were treated with LPS, TPCK (30  $\mu\text{M}$ ), and liriorelinol B dimethyl ether. The pro-inflammatory cytokines productions were evaluated through an ELISA kits (eBioscience, Inc., San Diego, USA). In brief,  $1 \times 10^5$  cells were seeded in 24-well plates for 24 h. The cells were pre-treated with several concentrations of liriorelinol B dimethyl ether or a vehicle for 2 h and then the macrophages were stimulated by LPS (1  $\mu\text{g}/\text{ml}$ ) for an additional 18 h. 100  $\mu\text{l}$  of the supernatant was transferred to 96-well culture plates and pro-inflammatory cytokines (TNF- $\alpha$ , IL-1 $\beta$ , IL-6) were determined according to the manufacturer's recommendations (eBioscience, Inc., San Diego, USA). For comparison, TPCK (30  $\mu\text{M}$ ) was used as a positive control [25,26].

### 2.11. Paw edema induced by carrageenan in mice

To assess the inhibitory effects of liriorelinol B dimethyl ether on inflammatory paw edema, animals were separated into four groups (vehicle control, dexamethasone - 50 mg per kg, liriorelinol B dimethyl ether - 10 mg per kg, and liriorelinol B dimethyl ether - 50 mg per kg) containing five mice each. Briefly, carrageenan (100  $\mu\text{g}$  per paw) was injected through the intraplantar (i.pl.) route for the induction of edema into the right hind paw [24,25,27]. Vehicle control mice received treatment with the vehicle (DMSO 2% in saline, i.pl) 1 h before the carrageenan challenge, and animals received an injection of saline, dexamethasone (50 mg per kg), or liriorelinol B dimethyl ether (10 or 50 mg per kg) intraperitoneally (i.p.). Paw thickness was measured after every 1 h for 5 h using a dial thickness gauge.

### 2.12. Determination of paw edema and mechanical hyperalgesia induced by CFA in mice

The liriorelinol B dimethyl ether was investigated for chronic CFA-induced mechanical hyperalgesia according to the Randall-Selitto method (Digital paw pressure Randall-Selitto meter, IITC Life Science Inc., Woodland Hills, USA) according to Khan et al. [23]. The animals were separated into three groups (vehicle control, dexamethasone - 20 mg per kg, and liriorelinol B dimethyl ether - 50 mg per kg) containing seven mice each. Briefly, a CFA-induced chronic effect of liriorelinol B dimethyl ether (50 mg/kg) was evaluated at intervals of day 0 to day 6 after the administration of drugs. The paw tissues were collected at day 6 after the CFA administration for further analysis. The end-point was the paw withdrawal in response to the pressure applied to the hind paw by a hand-held transducer. Three readings were taken for each animal and the average was noted as described previously

[23].

### 2.13. Molecular docking of liriorelinol B dimethyl ether on NF- $\kappa$ B inducing kinase (NIK)

Docking studies were performed using PyRx (version 0.8) Autodock Vina software. Molecular docking of liriorelinol B dimethyl ether was performed to determine their affinity with NF- $\kappa$ B-inducing kinase (NIK) with the AutoDock Vina (1.1.2).36 software. For the analysis, the tertiary structure of NF- $\kappa$ B was retrieved from the RCSB Protein Databank using the ID 4DN5. For the modification of proteins, Discovery Studio (version 4.1.0) was employed. The enzyme modification was conducted such that there were no chemical entities that could hamper ligand-protein binding in order to preserve the protein structure in pdb format. AutoDock Tools (version 1.5.6) was utilized. The search space was also maximized. For determining the binding potential of the ligands with the molecule, the protein was then saved in pdbqt format. The ligand, liriorelinol B dimethyl ether was downloaded, from Zinc. Organization and was saved in pdbqt format: a supported format for our docking software. After the protein and ligand files had been primed, docking was performed through AutoDock Vina. Output was expressed in binding energy (kcal/mol) [28].

### 2.14. Statistical analysis

Results were expressed as mean  $\pm$  standard deviation (SD) from three different experiments. For multiple comparisons, one-way analysis of variance (ANOVA) followed by Tukey's *post hoc* test was carried out. A value of  $P < 0.05$  was chosen as the criterion for statistical significance. In acute study five animals per group while, seven animals per group in chronic study were used. All statistical analyses were performed using the Statistical Package for the Social Sciences (SPSS), version 10.0 (IBM, Chicago, USA), and SigmaPlot, version 12.5 (Systat Software Inc., Chicago, USA).

## 3. Results

### 3.1. Effect of liriorelinol B dimethyl ether on cell viability, nitric oxide, and PGE<sub>2</sub> levels

To determine the effect of liriorelinol B dimethyl ether on cell viability, a MTT cell viability assay was performed (Fig. 1). The non-toxic concentration of liriorelinol B dimethyl ether was observed at 100  $\mu\text{M}$  (Fig. 1). Higher doses were not utilized because of the concern of introducing a higher concentration of DMSO. Therefore, the concentrations that were non-toxic (5, 15, 25, and 50  $\mu\text{M}$ ) were applied in further experiments.

Western immunoblot analysis was performed to evaluate the results of liriorelinol B dimethyl ether on the level of expression of iNOS and the COX-2 protein. iNOS protein expression level was remarkably inhibited by liriorelinol B dimethyl ether (Fig. 2). These result illustrated the inhibitory effect of liriorelinol B dimethyl ether on LPS-stimulated NO production by decreasing iNOS protein expression. The effect of liriorelinol B dimethyl ether on NO production was determined by Griess reagent. NO production was significantly elevated as a consequence of incubation with LPS alone in comparison to production in liriorelinol B dimethyl ether-treated LPS-induced RAW macrophages. Liriorelinol B dimethyl ether pretreatment prevented the increase in NO production in a dose-dependent manner (Fig. 2C). TPCK (30  $\mu\text{M}$ ) was used as a positive control in this experiment. A remarkable inhibition was found with 50  $\mu\text{M}$  liriorelinol B dimethyl ether.

Liriorelinol B dimethyl ether also dose-dependently suppressed LPS-induced COX-2 production in the media (Fig. 2B). PGE<sub>2</sub> production in control was reduced significantly in the media when treated with 25 and 50  $\mu\text{M}$  liriorelinol B dimethyl ether (Fig. 2D). This decrease in PGE<sub>2</sub> level was observed to be in strong agreement with COX-2 protein level.

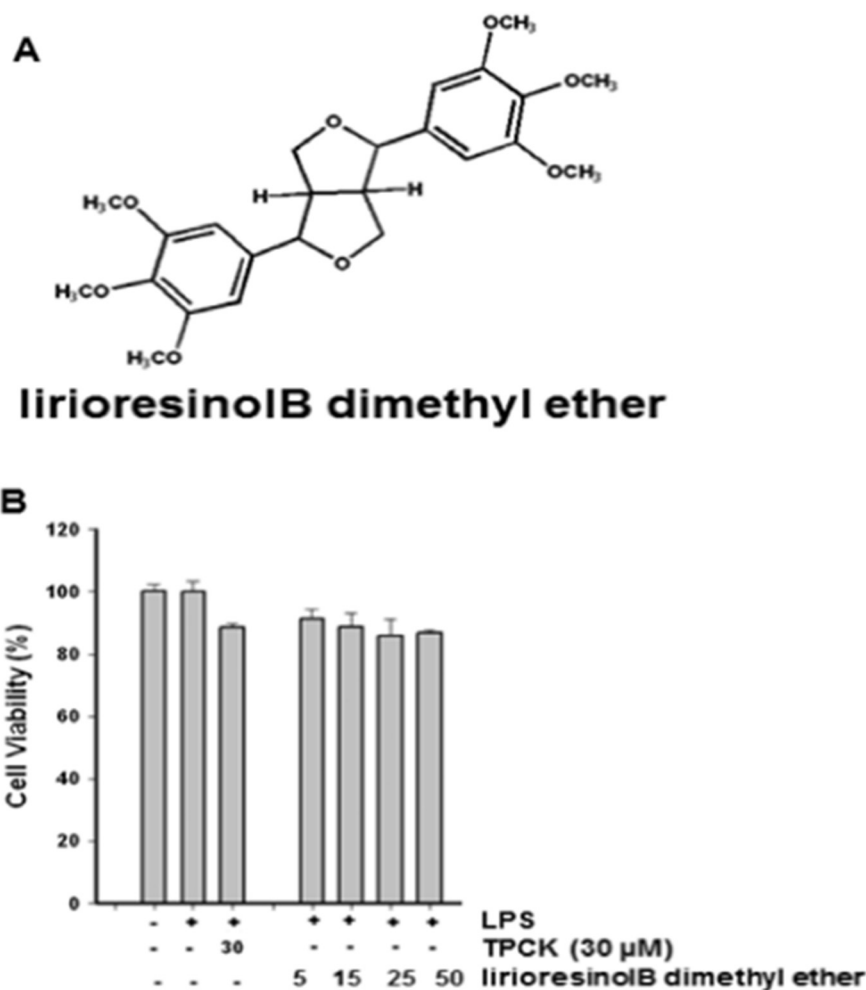


Fig. 1. (A) Chemical structure of liriioresinol B dimethyl ether. (B) Effect of liriioresinol B dimethyl ether on cell viability in RAW 264.7 macrophage cells stimulated with LPS.

Treatment with a positive control, celebrex (50 μM), also showed a remarkable reduction in PGE<sub>2</sub> level.

### 3.2. Liriioresinol B dimethyl ether inhibits the LPS-induced upstream MyD88/TLR4 signaling cascade and degradation of IκBα in macrophages

In order to determine the upstream effect of liriioresinol B dimethyl ether its effect on the level of TLR4 and its adaptor MyD88 was assessed. LPS exposure resulted in the upregulation of the expression levels of MyD88 and TLR4 (Fig. 3A–B). Treatment with liriioresinol B dimethyl ether exhibited an inhibition of signaling by downregulating MyD88 and TLR4 expression as stimulated by LPS. The Western blot analysis was performed to investigate the effect of liriioresinol B dimethyl ether on the degradation of IκBα (Fig. 3C). The activation and degradation of the IκBα protein is one of the main mechanism associated with the transcription of NF-κB. This allow release of free NF-κB and its translocation into the nucleus. Significant degradation of IκBα was observed after exposure of LPS alone (Fig. 3C). After 30 min of LPS exposure alone, IκBα was markedly reduced. Moreover, a rise in IκBα was observed with liriioresinol B dimethyl ether treatment (Fig. 3C).

### 3.3. Inhibitory effect of liriioresinol B dimethyl ether on LPS-induced MAPK pathway

The downstream effect of liriioresinol B dimethyl ether was assessed at the level of MAPK pathway. The MAPK pathway has an important role in the expression of pro-inflammatory mediators in macrophages

stimulated by LPS [29]. MAPK is also involved in NF-κB activation [30,31]. In order to determine the inhibitory effect of liriioresinol B dimethyl ether (50 μM) against the activation of MAPK pathway, the LPS-stimulated phosphorylation of MAPK proteins, such as JNK, ERK and p38 MAPK were observed in LPS-induced RAW 264.7 cells. Liriioresinol B dimethyl ether downregulated the LPS-stimulated triggering of p38, ERK, and JNK after 30 min of LPS induction (Fig. 4A–C), indicating inhibition of MAPK signaling pathway.

### 3.4. Effect of liriioresinol B dimethyl ether on NF-κB SEAP, NF-κB-, and AP-1-DNA-binding activity in LPS-stimulated macrophages

To determine the downstream effect of liriioresinol B dimethyl ether, the activity of various concentrations of the liriioresinol B dimethyl ether on the DNA-binding activity of NF-κB and AP-1 in RAW 264.7 cells stimulated with LPS, an EMSA was performed. A remarkable decrease in DNA-binding activity of NF-κB was observed with pretreatment through liriioresinol B dimethyl ether and parthenolide (Fig. 5A). Activation of AP-1 is modulated by the activation of the MAPK cascade [23]. Treatment with liriioresinol B dimethyl ether (50 μM) significantly inhibited AP-1-DNA-binding ability as shown in Fig. 5B. Parthenolide, is a sesquiterpene lactone and it is specific NF-κB-DNA binding inhibitor (30 μM) significantly inhibited AP-1-DNA-binding affinity [22].

In order to investigate the molecular mechanism of liriioresinol B dimethyl ether (5, 15, 25, and 50 μM), NF-κB signaling was assessed in LPS-induced macrophages (Fig. 5C). Detection of the activated NF-κB was conducted by determining NF-κB-dependent transcription in

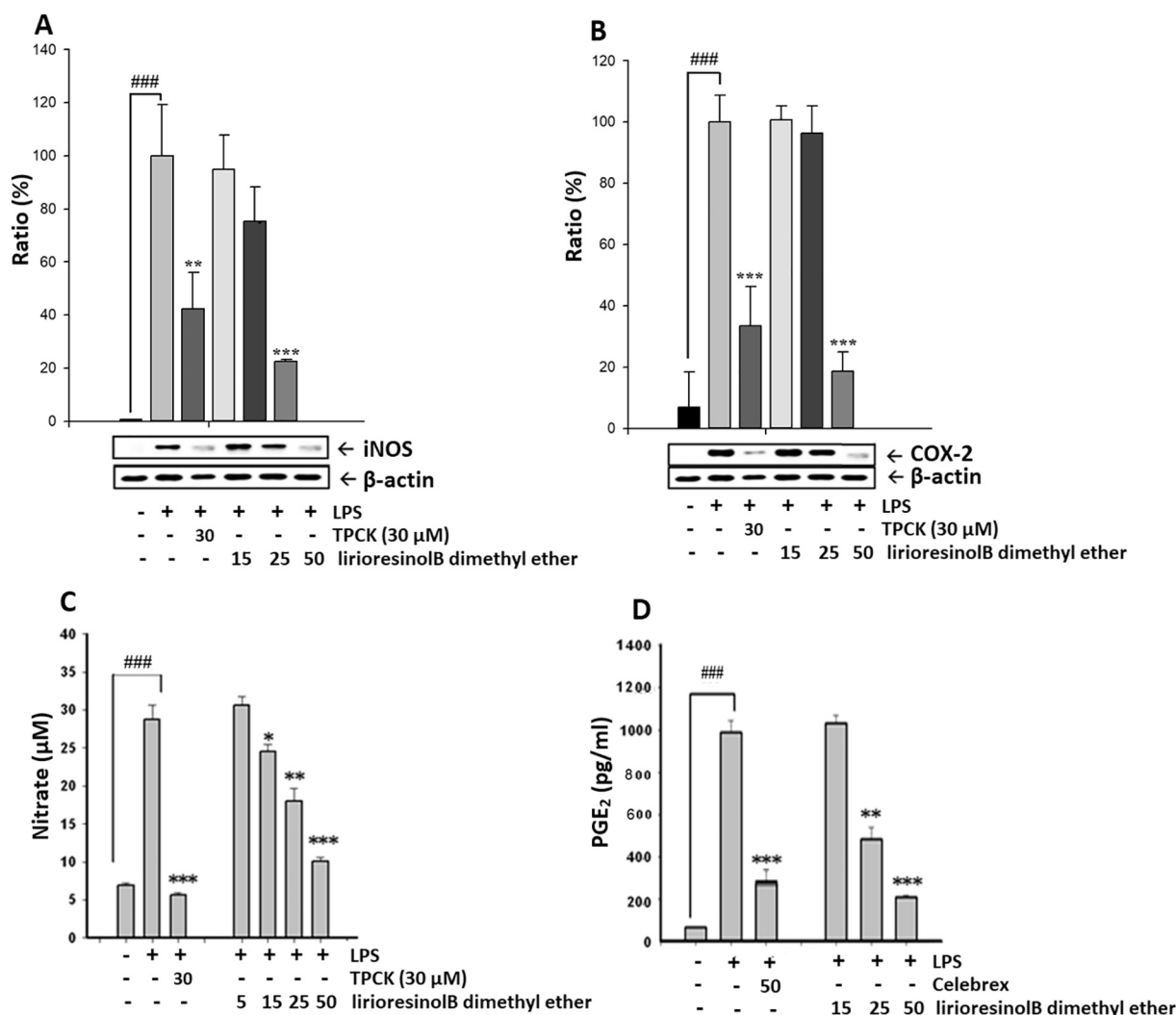


**Fig. 2.** Reduction in (A) iNOS and (B) COX-2 protein expression by liriioresinol B dimethyl ether in macrophages challenged with LPS assessed by using Western blotting. Effect of liriioresinol B dimethyl ether on (C) Nitrite production and (D) PGE<sub>2</sub> production using LPS-challenged RAW264.7 macrophages assessed by ELISA kit. The data was analyzed by multiple comparisons, one-way analysis of variance (ANOVA) followed by Tukey's *post hoc* test. Expressed as the mean ± S.D. from three different experiments. LPS (LPS + DMSO)-treated cells alone, TPCK (*N*-p-tosyl-L-phenylalanyl chloromethyl ketone) and celebrex served as positive controls. (\*) P < 0.05, (\*\*) P < 0.01 and (\*\*\*) P < 0.001 represents a remarkable difference from the LPS-stimulated group. ### P < 0.001 indicate a remarkable difference from the unstimulated control.

macrophages transfected with a luciferase reporter construct. A remarkable increase in NF-κB activity was detected by cells incubated with LPS alone, which was significantly inhibited by liriioresinol B dimethyl ether in a concentration-dependent manner (Fig. 5C). TPCK was used as a positive control, which extraordinarily suppressed LPS-induced increases in NF-κB activity.

**3.5. Inhibitory effect of liriioresinol B dimethyl ether on pro-inflammatory cytokines productions**

Additionally, to investigate the inhibitory effect of liriioresinol B dimethyl ether on pro-inflammatory cytokines productions (TNF-α, IL1β, and IL-6), an ELISA assay was performed (Fig. 5D–F). Liriioresinol B dimethyl ether markedly diminished the production of these cytokines in comparison to the LPS control. These results suggest the anti-inflammatory activity of liriioresinol B dimethyl ether.

**3.6. Effects of liriioresinol B dimethyl ether on carrageenan- and CFA-induced paw edema in mice**

In order to further explore the anti-inflammatory properties of

liriioresinol B dimethyl ether, a relationship between the *in vitro* and *in vivo* investigational models was established by performing acute and chronic paw inflammation models with carrageenan and CFA. To assess the acute anti-inflammatory properties of liriioresinol B dimethyl ether, carrageenan-induced paw edema was assessed throughout the investigational period (1, 2, 3, 4, and 5 h). The results indicated a major decrease in paw edema after carrageenan injection by liriioresinol B dimethyl ether (10, 50 mg/kg, i.p.), suggesting the inhibitory effect of liriioresinol B dimethyl ether in paw edema induced by carrageenan as depicted in Fig. 6A.

To evaluate the chronic anti-inflammatory and anti-hyperalgesic properties of liriioresinol B dimethyl ether, a CFA-induced chronic inflammatory model was performed. The results demonstrated that liriioresinol B dimethyl ether remarkably reduced paw edema and mechanical hyperalgesia in six days after CFA injection (Fig. 6B–C). Dexamethasone (positive control) also showed significant inhibition.

**3.7. Effect of liriioresinol B dimethyl ether in CFA-induced NF-κB and MAPK signaling in paw tissue**

The EMSA analysis demonstrated that liriioresinol B dimethyl ether

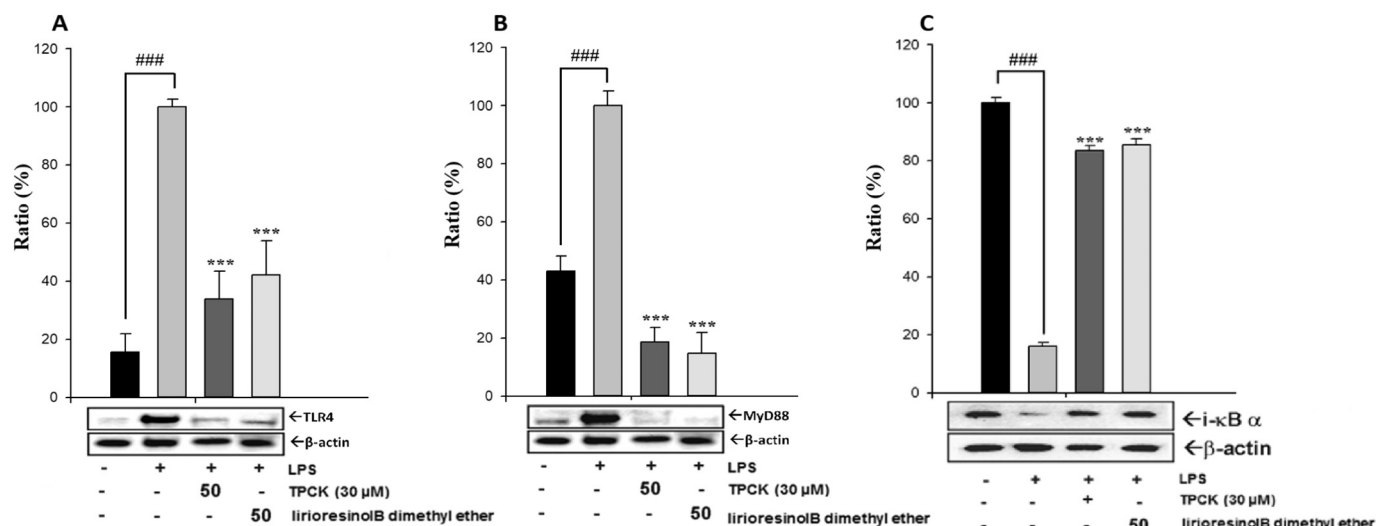


**Fig. 3.** Effect of lirioreosinol B dimethyl ether on the level of (A) TLR-4, (B) MyD88, and (C) IκBα protein expression in cytosolic extracts was analyzed by Western blot analysis. Data obtained from three separate experiments were analyzed by multiple comparisons, one-way analysis of variance (ANOVA) followed by Tukey's *post hoc* test and were expressed as the mean ± S.D. (\*\*\*)  $P < 0.001$  represents a remarkable difference from the LPS-stimulated group. ###  $P < 0.001$  represents a remarkable difference from the unstimulated control group. LPS (LPS + DMSO)-treated cells alone; 30 μM TPCK-a positive control.

remarkably inhibited NF-κB-DNA-binding affinity in CFA-induced paw tissue (Fig. 7A). To identify and specify further, the NF-κB subunits (p65 and p50) were established with Western blotting. The results showed that lirioreosinol B dimethyl ether significantly downregulated p65 and p50 (Fig. 7B–C). Meanwhile, CFA-induced paw tissue showed there to be a significant elevation in NF-κB subunits. Additionally, the MAPK proteins, such as c-jun and c-fos, were considerably downregulated by lirioreosinol B dimethyl ether (Fig. 7D–E).

### 3.8. Computational analysis of lirioreosinol B dimethyl ether for NF-κB inducing kinase (NIK)

To determine with more depth the mechanism underlying lirioreosinol B dimethyl ether, docking studies were performed as described in the Materials and Methods section. To examine the interaction of lirioreosinol B dimethyl ether and NF-κB at the active site (Fig. 8), the binding affinities of the enzyme-inhibitor complexes during docking

were calculated and found to be  $-4.474$  kcal/mol for 4DN5. The lower value reflected the more stable complex between the ligand and target protein. Further, this meant that lirioreosinol B dimethyl ether exhibited significantly stable binding with NF-κB. With lirioreosinol B dimethyl ether and 4DN5, there were hydrogen bonding interactions at Ser 476. The two-dimensional (2D) and three-dimensional (3D) images are presented in Fig. 8A and B, respectively.

## 4. Discussion

Natural compounds have played considerable roles as preventive and therapeutic agents for illnesses that have been known throughout human history [32,33]. In the present study, lirioreosinol B dimethyl ether was evaluated for its anti-inflammatory potential using macrophages stimulated with LPS and inflammatory mice models. Lirioreosinol B dimethyl ether significantly inhibited COX-2 and iNOS protein expressions and also inhibited PGE<sub>2</sub> and NO productions in a dose-

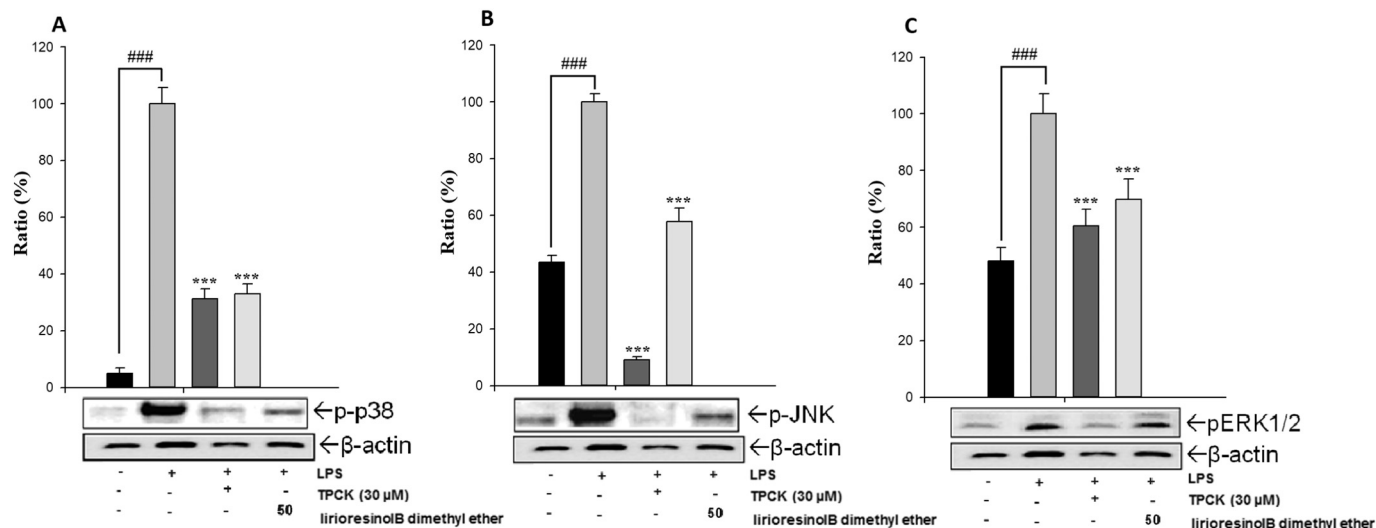


**Fig. 4.** Effect of lirioreosinol B dimethyl ether on the MAPK pathways, (A) p-p38, (B) p-ERK, and (C) p-JNK proteins in cytosolic extracts were assessed by Western blot analysis. Data obtained from three separate experiments were analyzed by multiple comparisons, one-way analysis of variance (ANOVA) followed by Tukey's *post hoc* test and were expressed as the mean ± S.D. (\*\*\*)  $P < 0.001$  represents a remarkable difference from the LPS-stimulated group. ###  $P < 0.001$  represents a remarkable difference from the unstimulated control group. LPS (LPS + DMSO)-treated cells alone; 30 μM TPCK-a positive control.



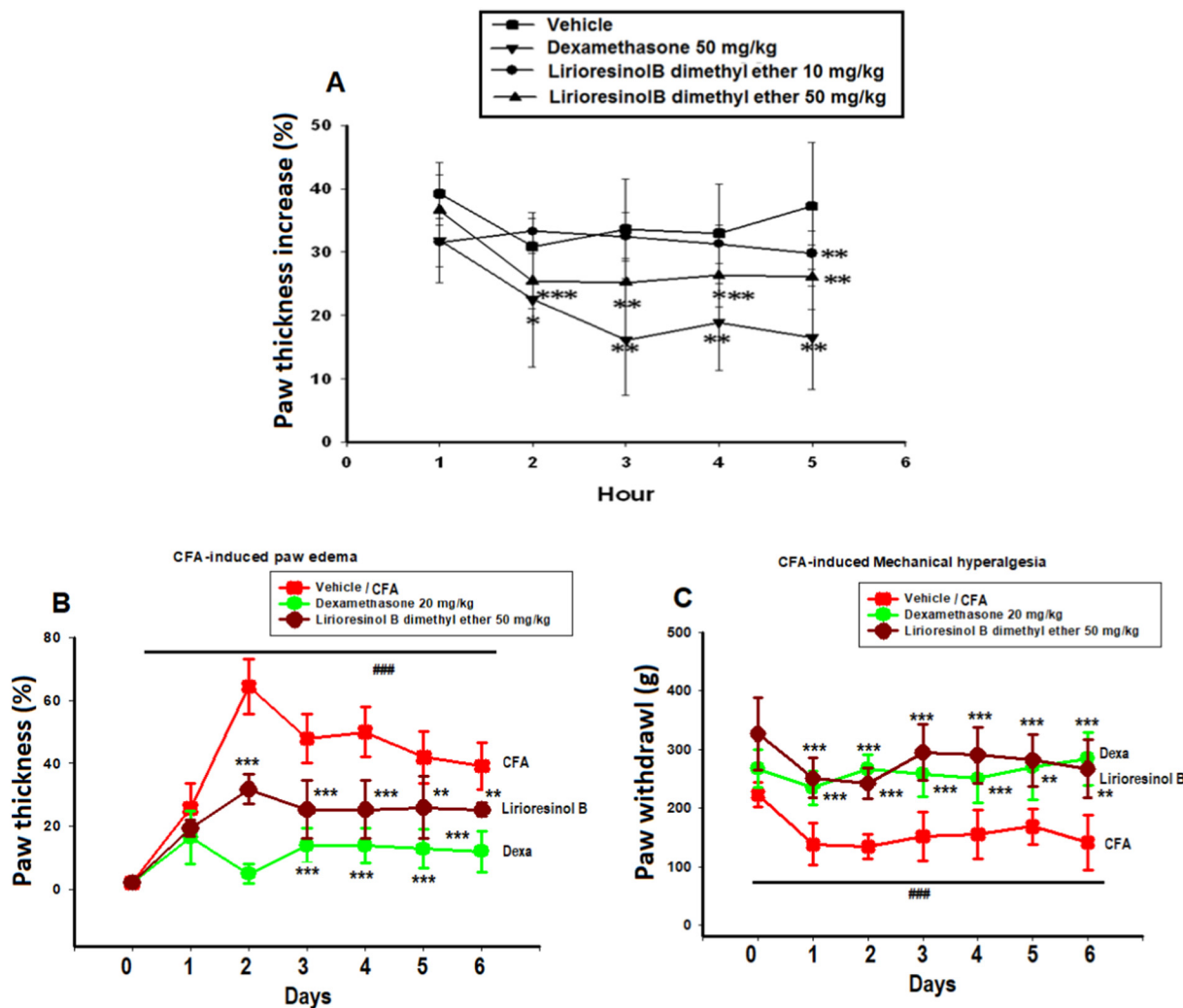


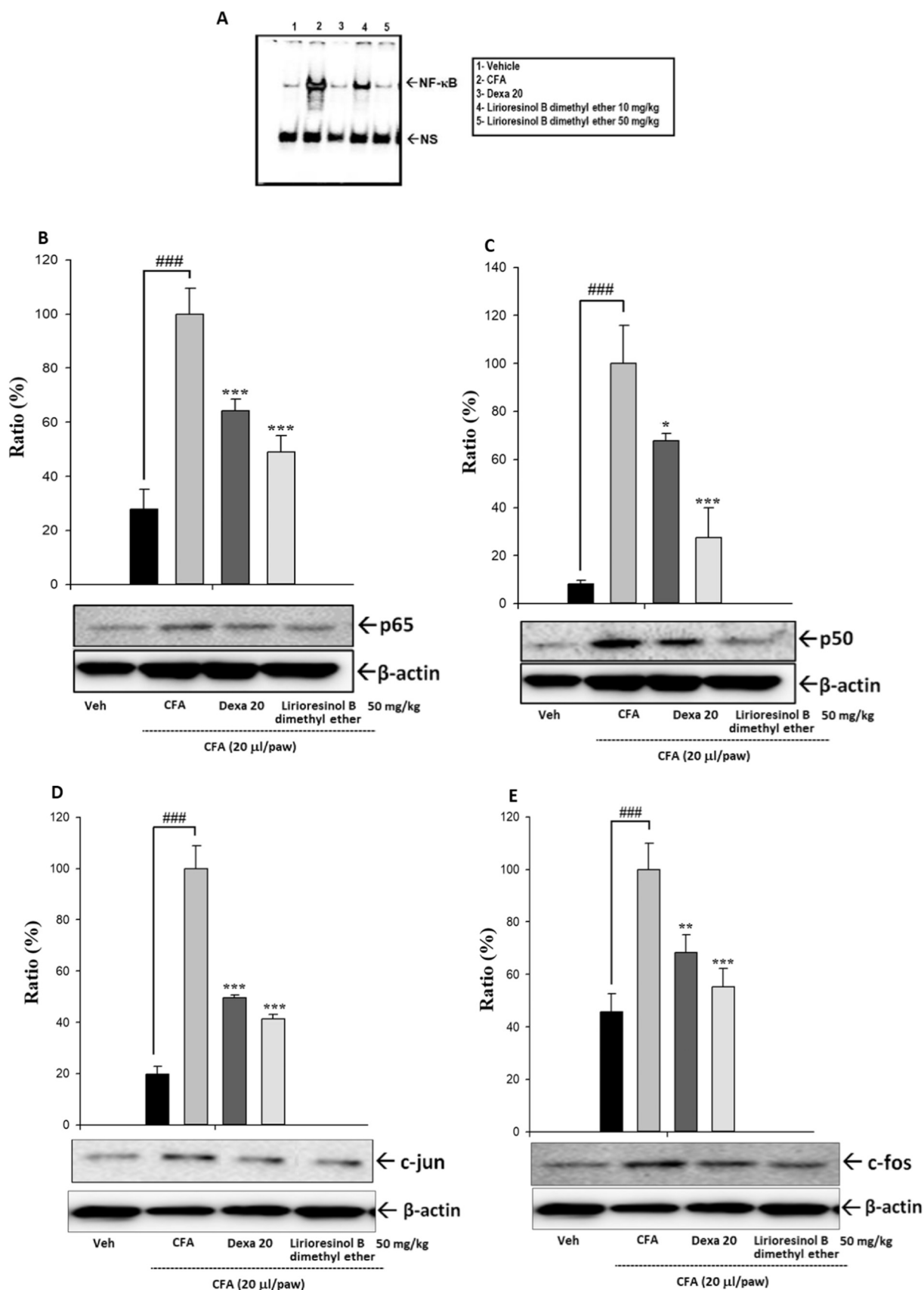
**Fig. 6.** Lirioresinol B dimethyl ether treatment inhibits (A) Carrageenan-induced paw edema. Paw edema was assessed every 1 h till 5 h after the carrageenan injection, (cm = %). (B) CFA-induced paw edema and (C) Mechanical hyperalgesia. Data were analyzed by multiple comparisons, one-way analysis of variance (ANOVA) followed by Tukey's *post hoc* test and was represented as mean ± S.D. per. (\*) P < 0.05, (\*\*) P < 0.01 and (\*\*\*) P < 0.001 represents a remarkable difference from the negative control group. ###P < 0.001 indicate a remarkable difference from the vehicle control.

dependent manner in LPS-induced RAW cells. These activities were shown in parallel with the reduction of I-κB phosphorylation, nuclear translocation of NF-κB, and suppression of AP-1 and MAPK proteins (p38, ERK, and JNK) activation.

Inflammatory responses are caused by the production of inflammatory mediators and cytokines, such as NO, PGE<sub>2</sub>, IL-1β, IL-6, and TNF-α [34,35]. The release of these molecules is a critical part of the immune response as a result of appropriate extracellular stimulation, such as stress or bacterial pathogens through TLRs [9]. Therefore, this study suggested that lirioresinol B dimethyl ether exhibits anti-inflammatory activity by inhibiting PGE<sub>2</sub> and NO productions stimulated by LPS, leading to the inhibition of COX-2 and iNOS expression via the NF-κB signaling cascade. Lirioresinol B dimethyl ether markedly suppressed the mediators of inflammation without changing cell viability of macrophages, which suggested that the anti-inflammatory activity of lirioresinol B dimethyl ether was not affected by any apparent cytotoxicity.

NF-κB is a crucial mediator of inflammatory processes [26]. Therefore, for the downregulation of inflammatory responses, inhibition of NF-κB within the immune system is an important therapeutic target. NF-κB controls the regulation and expression of pro-inflammatory genes by interacting and chemically modifying proteins, mostly from the I-κBα family [36]. Free NF-κB produced as a result of

phosphorylation of I-κBα translocates into the nucleus and initiates the transcription of target genes [37]. To study the mechanism of lirioresinol B dimethyl ether, LPS-induced NF-κB signaling pathways in macrophages were examined. Lirioresinol B dimethyl ether inhibition of LPS-stimulated NF-κB activation through inhibition of cytoplasmic degradation of I-κBα was also observed. This evidence suggests that the lirioresinol B dimethyl ether suppressed the expression of COX-2 and iNOS genes through inhibiting the activation of NF-κB. These results indicate that the major effect of lirioresinol B dimethyl ether on anti-inflammatory activity was through the NF-κB pathway. Furthermore, the DNA-binding activity of AP-1 and NF-κB by EMSA demonstrated a significant decrease by lirioresinol B dimethyl ether in nuclear extracts obtained from LPS-activated macrophages. Therefore, the blocking of the binding of these proteins with specific DNA sequences inhibits DNA/AP-1 and DNA/NF-κB complexes from recruiting inflammatory cytokines and enzymes, such as iNOS, COX-2, IL-6, IL-1β, and TNF-α. Additionally, TLR4 activated by LPS results in the initiation of specific intracellular pathways via dimerization of receptors and recruitment of numerous adaptor molecules, like TLR4 and MyD88 [38,39]. It has also been reported that NF-κB activation is stimulated by TLR4 signals through the MyD88/TLR4 pathway [40]. With this, the present study demonstrated a significant reduction of MyD88 and TLR4 protein expression by lirioresinol B dimethyl ether.



(caption on next page)

**Fig. 7.** Effects of liriioresinol B dimethyl ether on NF- $\kappa$ B DNA binding activity pathway in CFA-induced paw tissue. (A) A representative EMSA result is displayed indicating the NF- $\kappa$ B complexes, nonspecific signals (ns), and excessive probe. Effects of liriioresinol B dimethyl ether on NF- $\kappa$ B subunits (B) p65 and (C) p50. And MAPK pathway (D) c-jun, and (E) c-fos protein in CFA-induced paw tissue were assessed by Western blot analysis. Dexamethasone (20  $\mu$ M) used as positive control. Data were analyzed by multiple comparisons, one-way analysis of variance (ANOVA) followed by Tukey's *post hoc* test and was indicated as the mean  $\pm$  S.D. (\*) P < 0.05, (\*\*) P < 0.01, and (\*\*\*) P < 0.001 indicate remarkable differences from the CFA-challenged group. ###P < 0.001 indicates a significant difference from the unstimulated control.

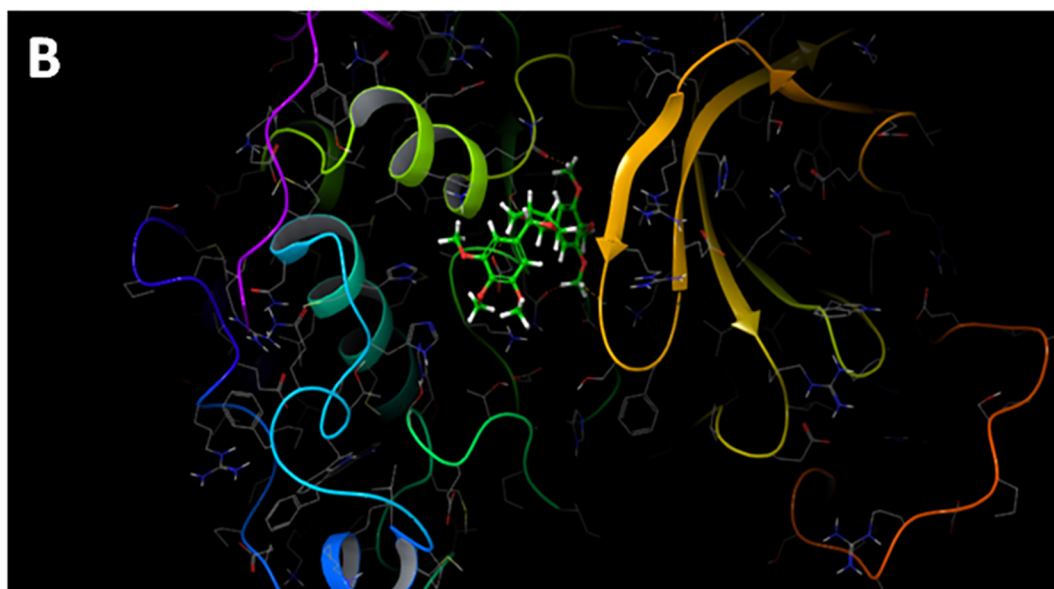
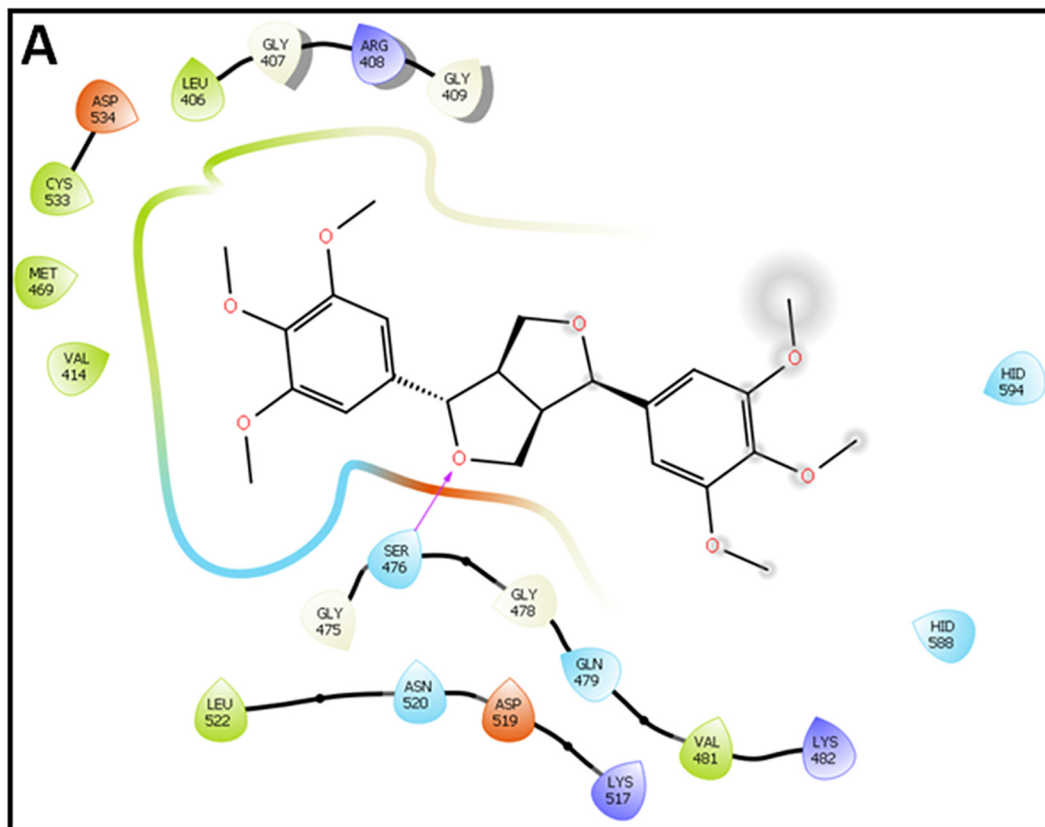


**Fig. 8.** Docking analysis of liriioresinol B dimethyl ether with NF- $\kappa$ B-inducing Kinase (NIK) (4DN5) depicting the ligand and protein interaction at the active site. (A) Two dimensional (2D) interaction between ligand and 4DN5. The legend represents the interaction type between the amino acid of the macromolecule and the ligand atoms. (B) Three-dimensional (3D) binding of liriioresinol B dimethyl ether with 4DN5. The secondary structure the protein is shown as a solid ribbon (green). Key residues are displayed in multicolor dots and lines, ligand is displayed in Multicolor. (For interpretation of the references to color in this figure legend, the reader is referred to the web version of this article.)

MAPK pathways regulate the expression of inflammatory cytokines and enzymes. Numerous studies have shown that anti-inflammatory agents alter gene expression by either MAPK-dependent or independent pathways [22,37]. The MAPKs activate transcriptional factors, like NF- $\kappa$ B and AP-1, through inflammatory and mitogenic signals, thereby inducing inflammatory genes [22]. MAPKs activate the expression of COX-2 and iNOS genes by NF- $\kappa$ B activation in LPS-stimulated macrophages [41]. The current experiments indicated the suppression of phosphorylation of JNK, p38, and ERK by liriioresinol B dimethyl ether. Overall, the study demonstrated the inhibitory effect of liriioresinol B dimethyl ether on LPS-activated production of NO through inactivation of NF- $\kappa$ B and AP-1 due to the suppression of phosphorylation of ERK, p38 MAPK, and JNK.

In order to explore the anti-inflammatory mechanism of liriioresinol B dimethyl ether, carrageenan- and CFA-induced inflammatory models were performed. Inflammation develops immediately after i.p. carrageenan injection, producing edema and hyperalgesia due to pro-inflammatory agents, including reactive oxygen, cytokines, bradykinin, and histamine [42,43]. I.p. administration of liriioresinol B dimethyl ether (10 and 50 mg per kg) 1 h prior to carrageenan injection remarkably reduced paw edema. Dexamethasone (50 mg per kg) also significantly inhibited paw edema induced by carrageenan. Similarly, liriioresinol B dimethyl ether diminished paw edema and mechanical hyperalgesia in chronic CFA models of inflammation. Furthermore, the behavior results were confirmed by analyzing NF- $\kappa$ B and MAPKs signaling in paw tissue. The results clearly demonstrated that liriioresinol B dimethyl ether inhibited both the signaling cascade by suppressing p65, p50, c-jun, and c-fos in CFA-induced paw tissue. So far, the study has some limitations that only male mice were used for *in vivo* analysis.

Docking studies of liriioresinol B dimethyl ether (50 mg/kg, i.p.) compound were carried out to assess the plausible binding interactions within the active site of NF- $\kappa$ B-inducing kinase. The enzyme modification was conducted such that there were no chemical entities that could hamper ligand-protein binding. The tertiary structure of NF- $\kappa$ B was retrieved from the RCSB Protein Databank using ID: 4DN5. To elucidate the interaction of liriioresinol B dimethyl ether and NF- $\kappa$ B at the active site, the binding affinities of the enzyme-inhibitor complexes were calculated to be  $-4.474$  kcal/mol for 4DN5. This value reflects a stable complex between the ligand and target protein. Putative binding interactions of the compound, liriioresinol B dimethyl ether (50 mg/kg, i.p.) within NIK are depicted in Fig. 8. Binding interactions of liriioresinol B dimethyl ether and co-crystallized ligand exhibit hydrogen-bonding interactions at Ser 476. Analysis of the binding interactions of liriioresinol B dimethyl ether revealed that compounds were efficiently docked inside the active site of the target structure, similar to that of the co-crystallized ligand.

In conclusion, the current study demonstrated that liriioresinol B dimethyl ether exerts remarkable inhibitory activity on the LPS-stimulated release of pro-inflammatory mediators both in *in vitro* and *in vivo*. This anti-inflammatory characteristic occurs through inhibition of the expression of COX-2 and iNOS via reduction in the activation of AP-1 and NF- $\kappa$ B transcription factors through MyD88/TIRAP. This suppression results from the inhibition of IKK phosphorylation, and also from the inhibition of degradation and phosphorylation of I $\kappa$ B $\alpha$ . Liriioresinol B dimethyl ether inhibited carrageenan- and CFA-induced inflammation through suppression of NF- $\kappa$ B and MAPK protein activation. Taken together, suppression of NF- $\kappa$ B and MAPK signaling pathway activation potentially could prevent inflammatory disorders.

## References

- [1] S. Khan, O. Shehzad, M.-S. Cheng, R.-J. Li, Y.S. Kim, Pharmacological mechanism underlying anti-inflammatory properties of two structurally divergent coumarins through the inhibition of pro-inflammatory enzymes and cytokines, *J. Inflamm.* 12 (1) (2015) 47.
- [2] M. Kaur, M. Singh, O. Silakari, Inhibitors of switch kinase 'spleen tyrosine kinase' in inflammation and immune-mediated disorders: a review, *Eur. J. Med. Chem.* 67 (2013) 434–446.
- [3] T. Owens, A.A. Babcock, J.M. Millward, H. Toft-Hansen, Cytokine and chemokine inter-regulation in the inflamed or injured CNS, *Brain Res. Rev.* 48 (2) (2005) 178–184.
- [4] A. Tosun, S. Khan, Y.S. Kim, Á. Calín-Sánchez, X. Hysenaj, A. Carbonell-Barrachina, Essential oil composition and anti-inflammatory activity of *Salvia officinalis* L. (Lamiaceae) in murin macrophages, *Trop. J. Pharm. Res.* 13 (6) (2014) 937–942.
- [5] L. Ferrero-Miliani, O. Nielsen, P. Andersen, S. Girardin, Chronic inflammation: importance of NOD2 and NALP3 in interleukin-1 $\beta$  generation, *Clinical & Experimental Immunology* 147 (2) (2007) 227–235.
- [6] M.Z. Ullah, A.U. Khan, R. Afridi, H. Rasheed, S. Khalid, M. Naveed, H. Ali, Y.S. Kim, S. Khan, Attenuation of inflammatory pain by puerarin in animal model of inflammation through inhibition of pro-inflammatory mediators, *Int. Immunopharmacol.* 61 (2018) 306–316.
- [7] B. Shal, A. Khan, M. Naveed, N. Ullah Khan, H. Ihsan Ul, S. DA, Y.S. Kim, S. Khan, Effect of 25-methoxy hispidol A isolated from *Poncirus trifoliata* against bacteria-induced anxiety and depression by targeting neuroinflammation, oxidative stress and apoptosis in mice, *Biomedicine & pharmacotherapy = Biomedecine & pharmacotherapie* 111 (2018) 209–223.
- [8] P. Datla, M.D. Kalluri, K. Basha, A. Bellary, R. Kshirsagar, Y. Kanekar, S. Upadhyay, S. Singh, V. Rajagopal, 9,10-dihydro-2,5-dimethoxyphenanthrene-1,7-diol, from *Eulophia ochreatea*, inhibits inflammatory signalling mediated by Toll-like receptors, *Br. J. Pharmacol.* 160 (5) (2010) 1158–1170.
- [9] J. Chun, R.J. Choi, S. Khan, D.-S. Lee, Y.-C. Kim, Y.-J. Nam, D.-U. Lee, Y.S. Kim, Alantolactone suppresses inducible nitric oxide synthase and cyclooxygenase-2 expression by down-regulating NF- $\kappa$ B, MAPK and AP-1 via the MyD88 signaling pathway in LPS-activated RAW 264.7 cells, *Int. Immunopharmacol.* 14 (4) (2012) 375–383.
- [10] S.M. Khan, R.J. Choi, D.U. Lee, Y.S. Kim, Sesquiterpene derivatives isolated from *Cyperus rotundus* L. inhibit inflammatory signaling mediated by NF- $\kappa$ B, *Nat. Prod. Sci.* 17 (3) (2011) 250–255.
- [11] H. Rasheed, R. Afridi, A.U. Khan, M.Z. Ullah, S. Khalid, A. Atiq, H. Kashif, M.N. Ahmed, Y.S. Kim, S. Khan, Anti-inflammatory, anti-rheumatic and analgesic activities of 2-(5-mercapto-1, 3, 4-oxadiazol-2-yl)-N-propylbenzenesulphonamide (MOPBS) in rodents, *Inflammopharmacology* (2018) 1–13.
- [12] N.M. Novotny, T.A. Markel, P.R. Crisostomo, D.R. Meldrum, Differential IL-6 and VEGF secretion in adult and neonatal mesenchymal stem cells: role of NF $\kappa$ B, *Cytokine* 43 (2) (2008) 215–219.
- [13] S. Khan, O. Shehzad, K.J. Lee, A. Tosun, Y.S. Kim, Anti-inflammatory properties of samidin from *Seseli resinosum* through suppression of NF- $\kappa$ B and AP-1-mediated genes in LPS-stimulated RAW 264.7 cells, *Arch. Pharm. Res.* 37 (11) (2014) 1496–1503.
- [14] E.-K. Kim, M.-Y. Song, I.-S. Kim, W.S. Moon, D.-G. Ryu, H.-S. So, R. Park, J.-W. Park, K.-B. Kwon, B.-H. Park, Beneficial effect of *Flos magnoliae* extract on multiple low dose streptozotocin-induced type 1 diabetes development and cytokine-induced  $\beta$ -cell damage, *Int. J. Mol. Med.* 22 (4) (2008) 481–488.
- [15] E.K. Kim, M.Y. Song, I.S. Kim, W.S. Moon, D.G. Ryu, H.S. So, R. Park, J.W. Park, K.B. Kwon, B.H. Park, Beneficial effect of *Flos magnoliae* extract on multiple low dose streptozotocin-induced type 1 diabetes development and cytokine-induced beta-cell damage, *Int. J. Mol. Med.* 22 (4) (2008) 481–488.
- [16] W. Schuhly, J. Skarbina, O. Kunert, O.I. Nandi, R. Bauer, Chemical characterization of *Magnolia biondii* (*Flos Magnoliae*, Xin Yi), *Nat. Prod. Commun.* 4 (2) (2009) 231–234.
- [17] W.-S. Feng, Y.-H. He, X.-K. Zheng, J.-C. Wang, Y.-G. Cao, Y.-L. Zhang, K. Song, Four new monoterpenoid glycosides from the flower buds of *Magnolia biondii*, *Molecules (Basel, Switzerland)* 21(6) (2016) 728.
- [18] A.Y. Jun, H.J. Kim, K.K. Park, K.H. Son, D.H. Lee, M.H. Woo, W.Y. Chung, Tetrahydrofuran-type lignans inhibit breast cancer-mediated bone destruction by blocking the vicious cycle between cancer cells, osteoblasts and osteoclasts, *Investig. New Drugs* 32 (1) (2014) 1–13.
- [19] C.D. Hufford, M.J. Funderburk, J.M. Morgan, L.W. Robertson, Two antimicrobial alkaloids from heartwood of *Liriodendron tulipifera* L, *J. Pharm. Sci.* 64 (5) (1975) 789–792.
- [20] Y.H. Kim, S.H. Lee, J.Y. Lee, S.W. Choi, J.W. Park, T.K. Kwon, Triptolide inhibits murine-inducible nitric oxide synthase expression by down-regulating lipopolysaccharide-induced activity of nuclear factor-kappa B and c-Jun NH2-terminal kinase, *Eur. J. Pharmacol.* 494 (1) (2004) 1–9.
- [21] S. Khan, E.M. Shin, R.J. Choi, Y.H. Jung, J. Kim, A. Tosun, Y.S. Kim, Suppression of LPS-induced inflammatory and NF-kappaB responses by anomalin in RAW 264.7 macrophages, *J. Cell. Biochem.* 112 (8) (2011) 2179–2188.
- [22] S. Khan, O. Shehzad, H.G. Jin, E.R. Woo, S.S. Kang, S.W. Baek, J. Kim, Y.S. Kim, Anti-inflammatory mechanism of 15,16-epoxy-3 $\alpha$ -hydroxylabda-8,13(16),14-trien-7-one via inhibition of LPS-induced multicellular signaling pathways, *J. Nat. Prod.* 75 (1) (2012) 67–71.
- [23] S. Khan, O. Shehzad, J. Chun, Y.S. Kim, Mechanism underlying anti-hyperalgesic and anti-allodynic properties of anomalin in both acute and chronic inflammatory pain models in mice through inhibition of NF-kappaB, MAPKs and CREB signaling cascades, *Eur. J. Pharmacol.* 718 (1–3) (2013) 448–458.
- [24] E.M. Shin, H.Y. Zhou, G.H. Xu, S.H. Lee, I. Merfort, Y.S. Kim, Anti-inflammatory activity of hispidol A 25-methyl ether, a triterpenoid isolated from *Poncirus Fructus*, *Eur. J. Pharmacol.* 627 (1–3) (2010) 318–324.
- [25] S. Khalid, M.Z. Ullah, A.U. Khan, R. Afridi, H. Rasheed, A. Khan, H. Ali, Y.S. Kim, S. Khan, Antihyperalgesic properties of honokiol in inflammatory pain models by targeting of NF- $\kappa$ B and Nrf2 signaling, *Front. Pharmacol.* 9 (2018) 140.
- [26] S. Khan, O. Shehzad, J. Chun, Y.S. Kim, Mechanism underlying anti-hyperalgesic and anti-allodynic properties of anomalin in both acute and chronic inflammatory

- pain models in mice through inhibition of NF- $\kappa$ B, MAPKs and CREB signaling cascades, *Eur. J. Pharmacol.* 718 (1) (2013) 448–458.
- [27] K.A. da Silva, M.N. Manjavachi, A.F. Paszcuk, M. Pivatto, C. Viegas Jr., V.S. Bolzani, J.B. Calixto, Plant derived alkaloid (-)-cassine induces anti-inflammatory and anti-hyperalgesic effects in both acute and chronic inflammatory and neuropathic pain models, *Neuropharmacology* 62 (2) (2012) 967–977.
- [28] A. Khan, M.Z. Ullah, R. Afridi, H. Rasheed, S. Khalid, H. Ullah, H. Ali, S.D. AlSharari, Y.S. Kim, S. Khan, Antinociceptive properties of 25-methoxy hispidol A, a triterpenoid isolated from *Poncirus trifoliata* (Rutaceae) through inhibition of NF-kappaB signalling in mice, *Phytotherapy research: PTR* 33 (2) (2019) 327–341.
- [29] S.M. Khan, Y.S. Kim, Reviews: molecular mechanism of inflammatory signaling and predominant role of *Saposhnikovia divaricata* as anti-inflammatory potential, *Nat. Prod. Sci.* 19 (2) (2013) 120–126.
- [30] C.S. Lai, J.H. Lee, C.T. Ho, C.B. Liu, J.M. Wang, Y.J. Wang, M.H. Pan, Rosmanol potentially inhibits lipopolysaccharide-induced iNOS and COX-2 expression through downregulating MAPK, NF-kappaB, STAT3 and C/EBP signaling pathways, *J. Agric. Food Chem.* 57 (22) (2009) 10990–10998.
- [31] H.G. Kim, D.H. Yoon, W.H. Lee, S.K. Han, B. Shrestha, C.H. Kim, M.H. Lim, W. Chang, S. Lim, S. Choi, W.O. Song, J.M. Sung, K.C. Hwang, T.W. Kim, *Phellinus linteus* inhibits inflammatory mediators by suppressing redox-based NF-kappaB and MAPKs activation in lipopolysaccharide-induced RAW 264.7 macrophage, *J. Ethnopharmacol.* 114 (3) (2007) 307–315.
- [32] F.E. Koehn, G.T. Carter, The evolving role of natural products in drug discovery, *Nat. Rev. Drug Discov.* 4 (3) (2005) 206.
- [33] B. Shal, W. Ding, H. Ali, Y.S. Kim, S. Khan, Anti-neuroinflammatory potential of natural products in attenuation of Alzheimer's disease, *Front. Pharmacol.* 9 (2018).
- [34] R.J. Choi, J. Chun, S. Khan, Y.S. Kim, Desoxyrhapontigenin, a potent anti-inflammatory phytochemical, inhibits LPS-induced inflammatory responses via suppressing NF- $\kappa$ B and MAPK pathways in RAW 264.7 cells, *Int. Immunopharmacol.* 18 (1) (2014) 182–190.
- [35] S. Khan, O. Shehzad, H.-G. Jin, E.-R. Woo, S.S. Kang, S.W. Baek, J. Kim, Y.S. Kim, Anti-inflammatory mechanism of 15, 16-epoxy-3 $\alpha$ -hydroxy- $\lambda$ -8, 13 (16), 14-trien-7-one via inhibition of LPS-induced multicellular signaling pathways, *J. Nat. Prod.* 75 (1) (2012) 67–71.
- [36] A. Hoffmann, A. Levchenko, M.L. Scott, D. Baltimore, The  $\kappa$ B-NF- $\kappa$ B signaling module: temporal control and selective gene activation, *Science* 298 (5596) (2002) 1241–1245.
- [37] H.-J. Lee, K. Maeng, G.-J. Kang, C. Ryou, J.H. Jung, H.-K. Kang, J.T. Prchal, E.-S. Yoo, D. Yoon, Anti-inflammatory effect of methyl dehydrojasmonate (J2) is mediated by the NF- $\kappa$ B pathway, *J. Mol. Med.* 89 (1) (2011) 83–90.
- [38] K.A. Fitzgerald, E.M. Palsson-McDermott, A.G. Bowie, C.A. Jefferies, A.S. Mansell, G. Brady, E. Brint, A. Dunne, P. Gray, M.T. Harte, D. McMurray, D.E. Smith, J.E. Sims, T.A. Bird, L.A. O'Neill, Mal (MyD88-adaptor-like) is required for Toll-like receptor-4 signal transduction, *Nature* 413 (6851) (2001) 78–83.
- [39] T. Horng, G.M. Barton, R. Medzhitov, TIRAP: an adapter molecule in the Toll signaling pathway, *Nat. Immunol.* 2 (9) (2001) 835–841.
- [40] T. Kawai, O. Takeuchi, T. Fujita, J. Inoue, P.F. Muhlradt, S. Sato, K. Hoshino, S. Akira, Lipopolysaccharide stimulates the MyD88-independent pathway and results in activation of IFN-regulatory factor 3 and the expression of a subset of lipopolysaccharide-inducible genes, *J. Immunol.* 167 (10) (2001) 5887–5894.
- [41] J.K. Kundu, Y.J. Surh, Breaking the relay in deregulated cellular signal transduction as a rationale for chemoprevention with anti-inflammatory phytochemicals, *Mutat. Res.* 591 (1–2) (2005) 123–146.
- [42] E.M. Shin, H.Y. Zhou, G.H. Xu, S.H. Lee, I. Merfort, Y.S. Kim, Anti-inflammatory activity of hispidol A 25-methyl ether, a triterpenoid isolated from *Poncirus Immaturus Fructus*, *Eur. J. Pharmacol.* 627 (1–3) (2010) 318–324.
- [43] S. Khan, O. Shehzad, J. Chun, R.J. Choi, S. Park, M.N. Islam, J.S. Choi, Y.S. Kim, Anti-hyperalgesic and anti-allodynic activities of capillarisin via suppression of inflammatory signaling in animal model, *J. Ethnopharmacol.* 152 (3) (2014) 478–486.